

## Supporting Information

### **Multi-wavelength excited triplet-triplet upconversion microcrystals based on hot-band excitation for optical information encryption**

Xiaofen Gu,<sup>‡</sup> Shuoran Chen,<sup>‡\*</sup> Zuoqin Liang, Xiaolei Ju, Lin Li, Xiaomei Wang and Changqing Ye\*

*Research Center for Green Printing Nanophotonic Materials, Suzhou Key Laboratory of New Energy Materials and Low Carbon Technologies, School of Materials Science and Engineering, Suzhou University of Science and Technology, Suzhou, 215009, China.*

<sup>‡</sup> These authors contributed equally to this work.

### **Corresponding Author**

E-mail: chensr@mail.usts.edu.cn; yechangqing@mail.usts.edu.cn

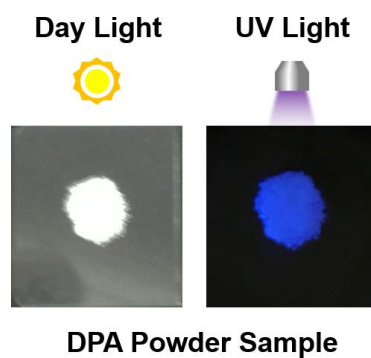


**Fig. S1** Photographs of the fluorescence of DPA microcrystals, under natural light and under irradiation of UV, respectively.

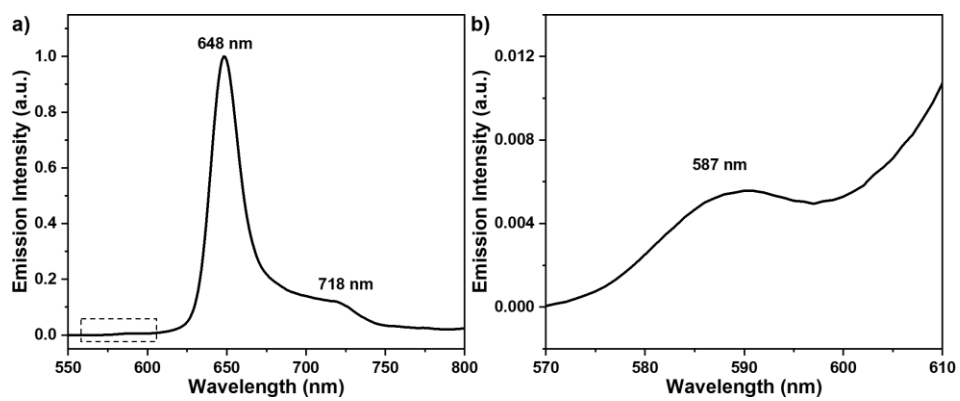


**Fig. S2** The emission spectrum of PtOEP (CHCl<sub>3</sub>, 10 μM), under the excitation of 536 nm in the air (r.t.).

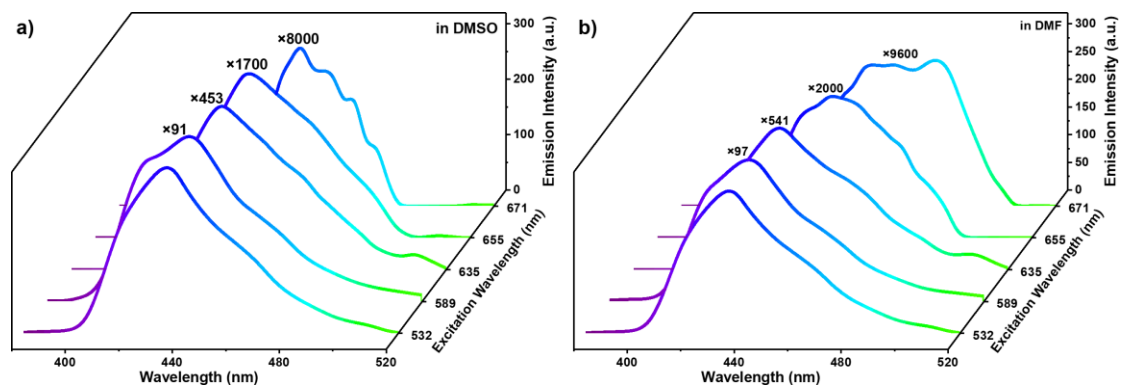


**Fig. S3** At power density of  $968 \text{ mW} \cdot \text{cm}^{-2}$ , the UC spectra of PtOEP/DPA ( $50 \mu\text{M}/1.4 \text{ mM}$ ) in (a) DMSO and in (b) DMF, under the excitation of 532 nm, 589 nm, 635 nm, 655 nm and 671 nm.

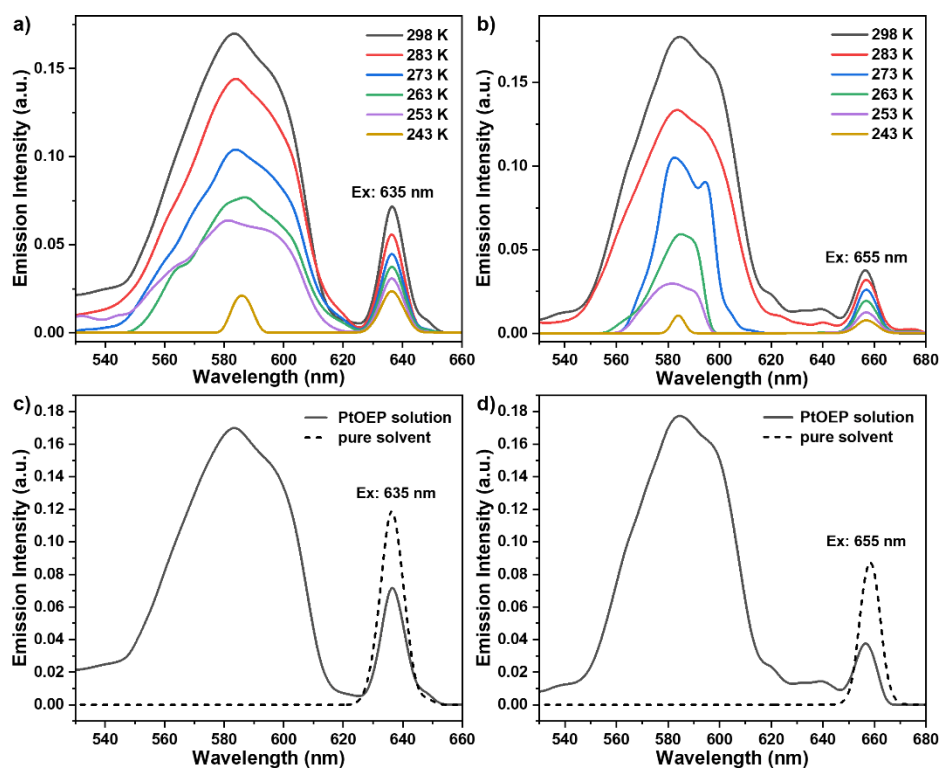


**Fig. S4** Temperature-dependent OPA-UC spectra of PtOEP (200  $\mu$ M, in  $\text{CHCl}_3$ , without degassing), under the excitation of (a) 635 nm diode laser and (b) 655 nm diode laser at 968  $\text{mW}/\text{cm}^2$ . PL spectra of pure solvent  $\text{CHCl}_3$  without any dyes and PtOEP solution excited at (c) 635 nm and (d) 655 nm.

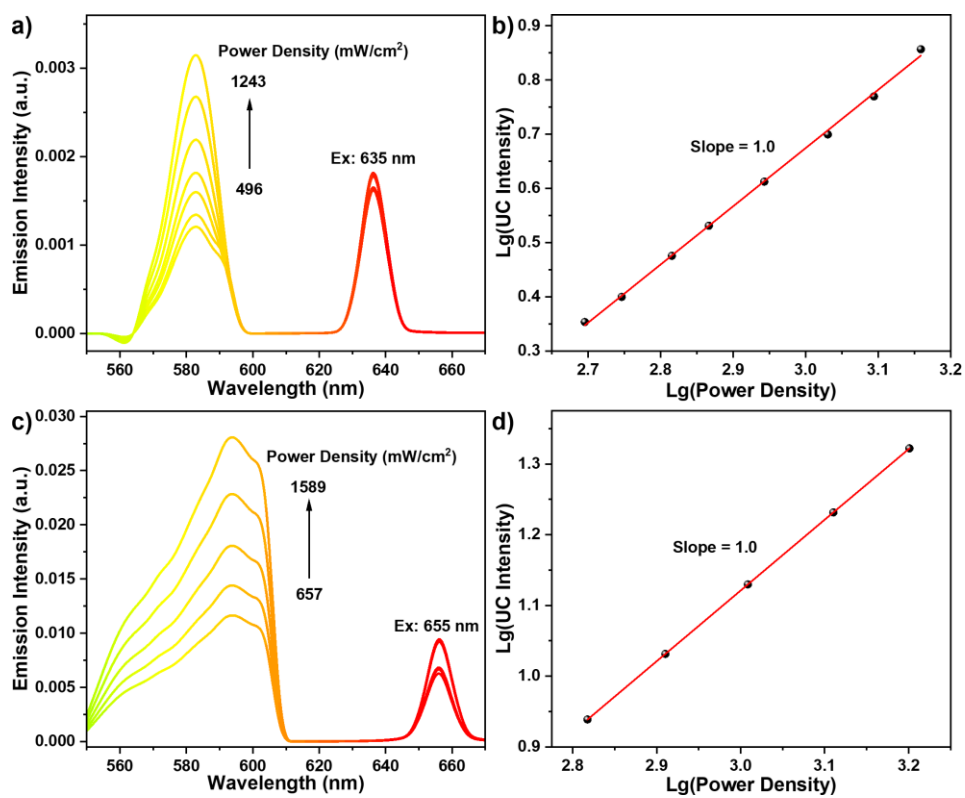


**Fig. S5** Power-dependent OPA-UC spectra of PtOEP (200  $\mu\text{M}$ , in  $\text{CHCl}_3$ , without degassing) and the corresponding logarithm relationship of OPA-UC integral intensity versus power density, under the excitation of (a,b) 635 nm and (c,d) 655 nm.

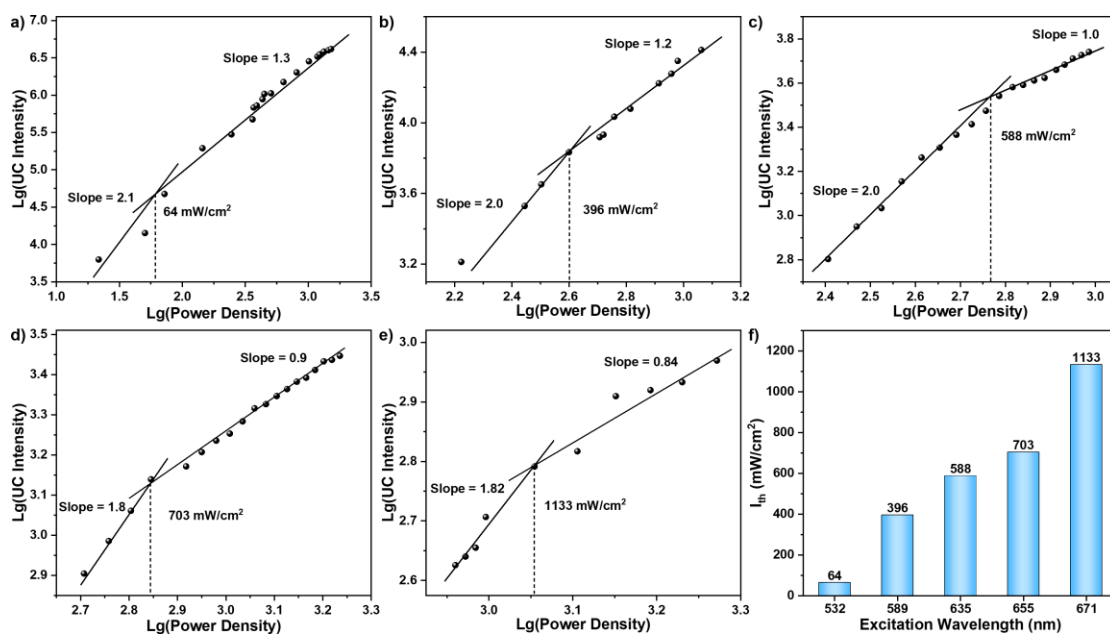


**Fig. S6** Logarithm relationships of UC emission integral intensity versus power densities (PtOEP/DPA: 50  $\mu$ M/1.4 mM, in degassed  $\text{CHCl}_3$ ), under the excitation of (a) 532 nm, (b) 589 nm, (c) 635 nm, (d) 655 nm and (e) 671 nm. (f) Histogram of the power density thresholds under different excitation wavelengths.

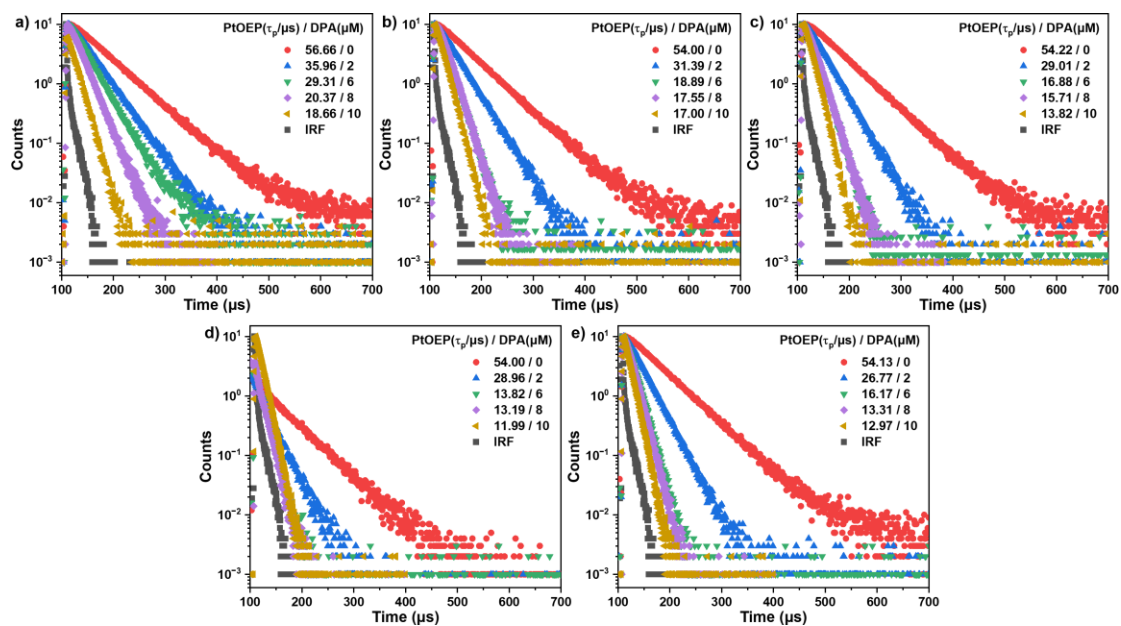


**Fig. S7** Time-resolved phosphorescence decay curves of PtOEP (50  $\mu\text{M}$ ,  $\text{CHCl}_3$ ) at 648 nm, with the DPA concentration increasing from 0, 2, 6, 8, to 10  $\mu\text{M}$ , under the excitation of (a) 532 nm, (b) 589 nm, (c) 635 nm, (d) 655 nm and (e) 671 nm.



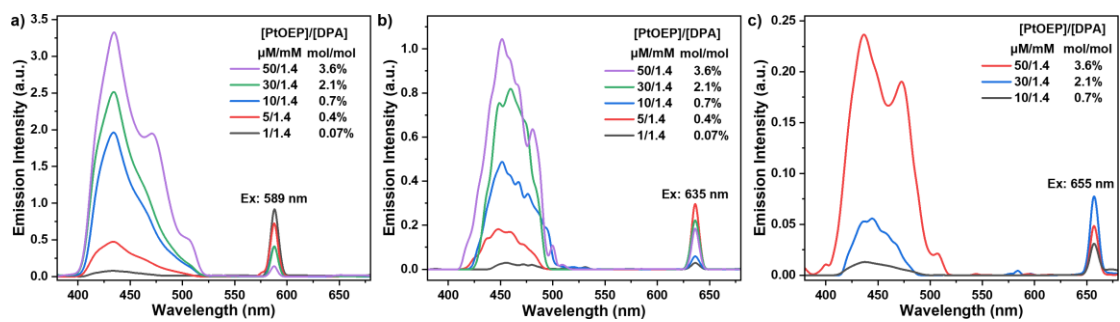


**Fig. S8** The hot-band excited TTA-UC spectra with DPA concentration fixed at 1.4 mM as the PtOEP concentration changes.

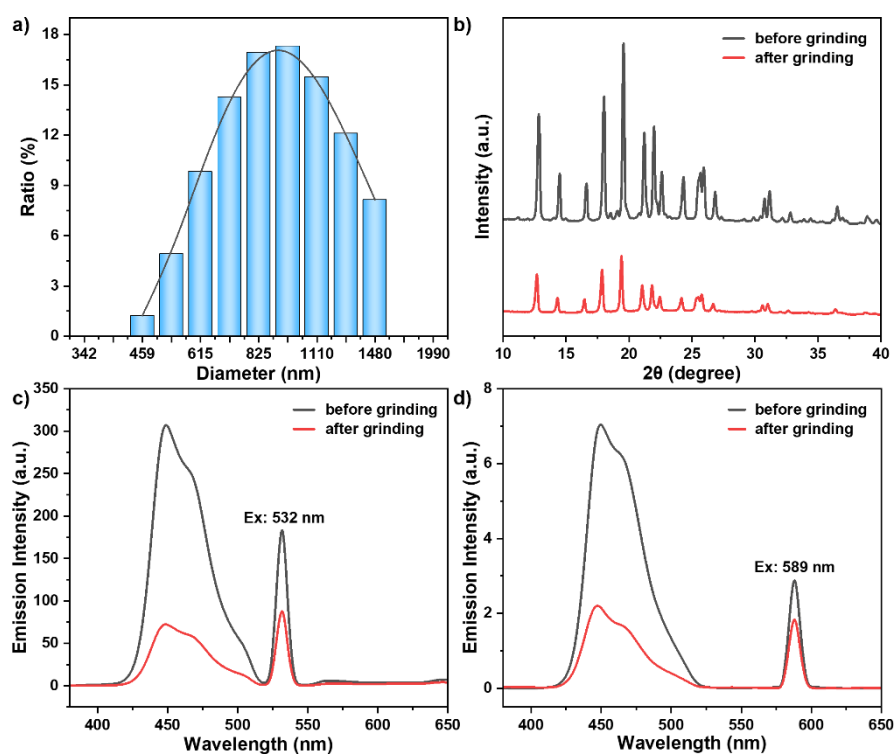


**Fig. S9** (a) Particle size distribution of the ground 1/12000 doped microcrystals; (b) PXRD spectrum of the 1/12000 doped microcrystals before (up) and after (down) grinding; (c-d) Emission spectra of the 1/12000 doped microcrystals before (black) and after (red) grinding, under (c) 532 nm and (d) 589 nm excitation ( $986 \text{ mW}\cdot\text{cm}^{-2}$ ) in a nitrogen atmosphere.

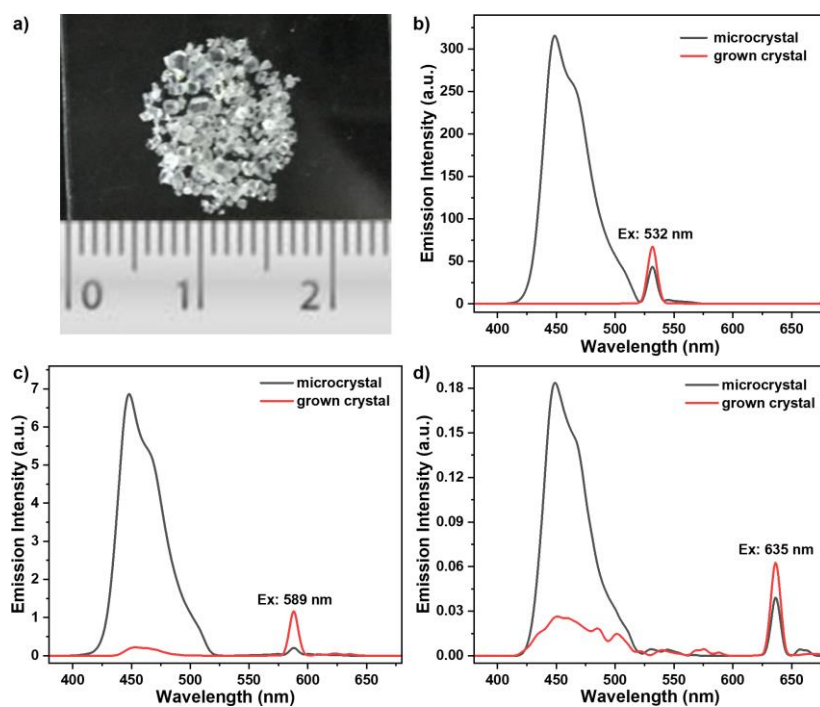


**Fig. S10** (a) Photo of the 1/12000 doped microcrystals grown into submillimeter crystals. The corresponding emission spectra under the excitation of (b) 532 nm, (c) 589 nm and (d) 635 nm at the same power density of  $968 \text{ mW}\cdot\text{cm}^{-2}$ . The emission spectra (black curves in b~d) of the 1/12000 doped microcrystals were also presented for comparison.

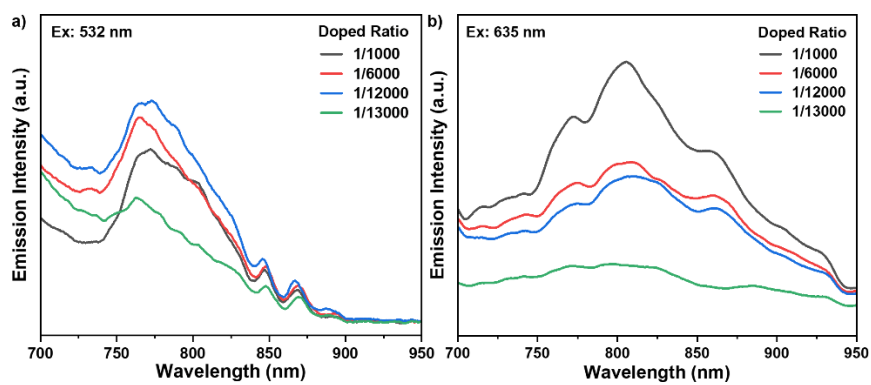


**Fig. S11** The emission spectra (above 700 nm) of the PtOEP/DPA microcrystals with different doped ratios (mol/mol), under the excitation of (a) 532 nm and (b) 635 nm, at a unique excitation power density of  $968 \text{ mW}\cdot\text{cm}^{-2}$ .

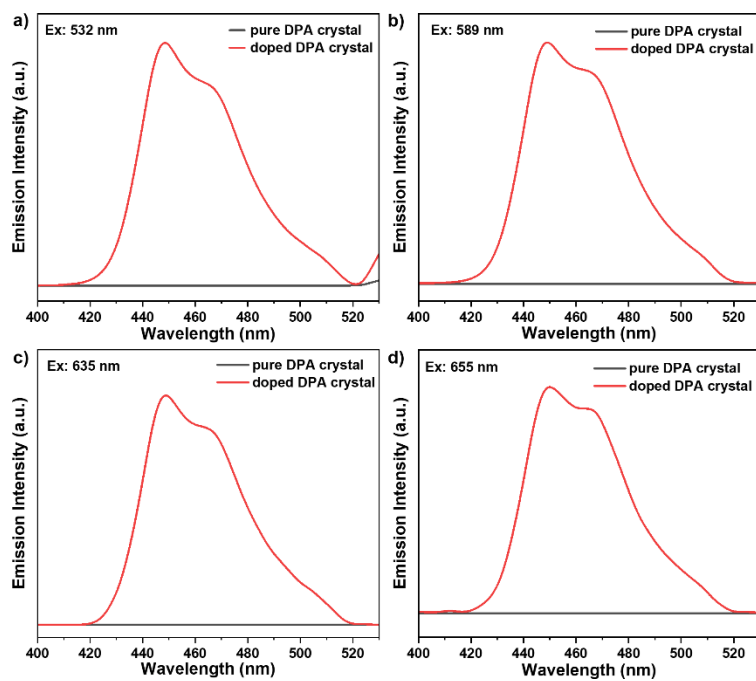


**Fig. S12** The emission spectra of the pure DPA and PtOEP doped DPA microcrystals under the excitation of (a) 532 nm, (b) 589 nm, (c) 635 nm and (d) 655 nm at a unique excitation power density of  $968 \text{ mW}\cdot\text{cm}^{-2}$ .

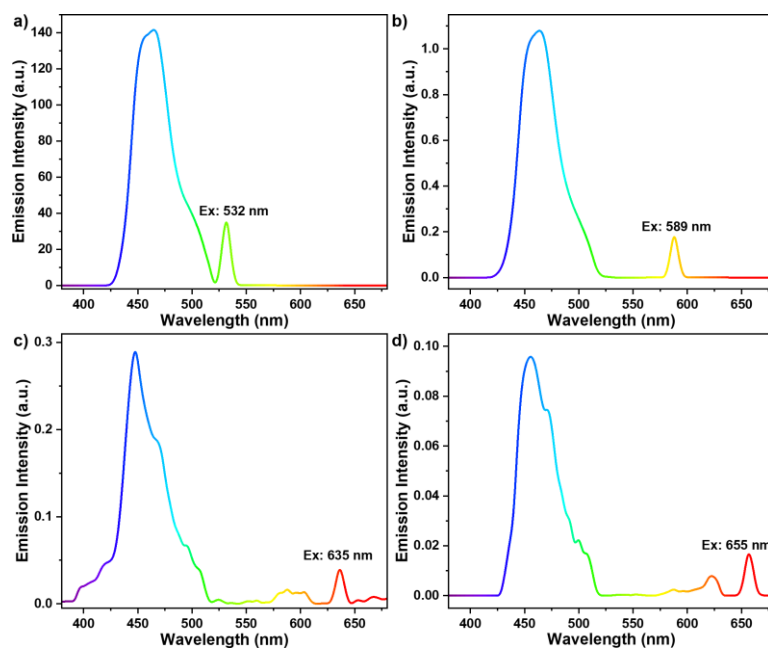


**Fig. S13** The emission spectra of 1/100000 doped microcrystals under different excitation wavelengths from (a) 532 nm, (b) 589 nm, (c) 635 nm and (d) 655 nm diode lasers at  $968 \text{ mW}\cdot\text{cm}^{-2}$ .

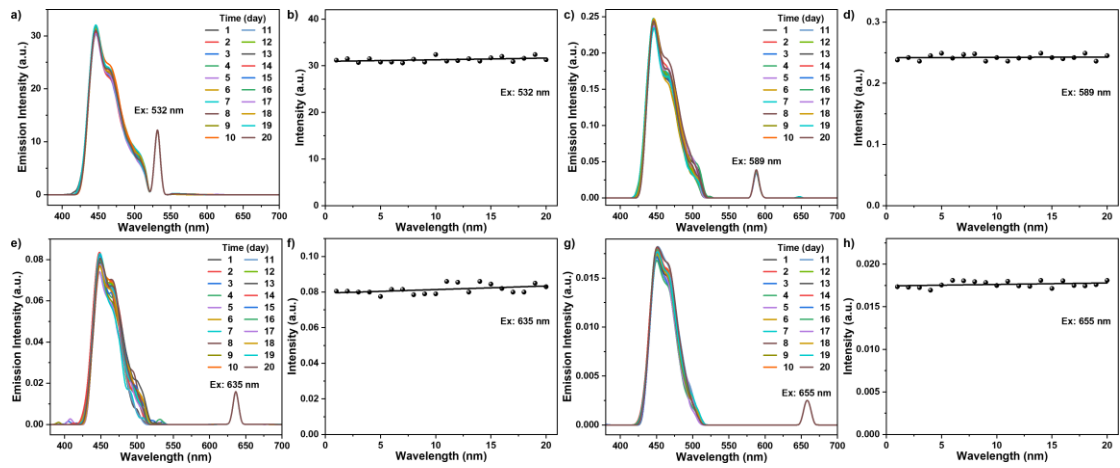


**Fig. S14** At power density at  $968 \text{ mW}\cdot\text{cm}^{-2}$ , the changes of emission spectra and UC intensity of 1/1000 doped microcrystals, under excitation of (a,b) 532 nm, (c,d) 589 nm, (e,f) 635 nm and (g,h) 655 nm through for 20 days (under the air atmosphere).

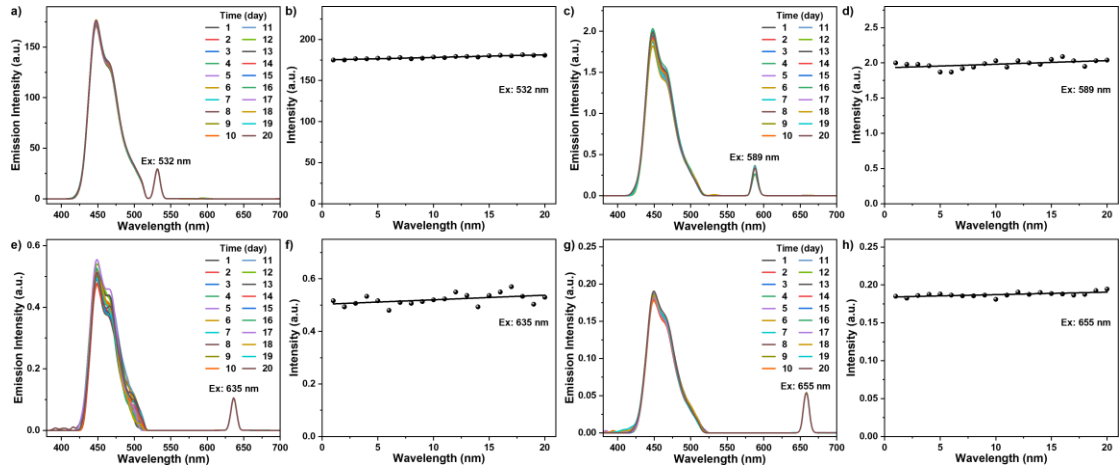


**Fig. S15** At power density at  $968 \text{ mW}\cdot\text{cm}^{-2}$ , the changes of emission spectra and UC intensity of 1/6000 doped microcrystals, under excitation of (a,b) 532 nm, (c,d) 589 nm, (e,f) 635 nm and (g,h) 655 nm through for 20 days (under the air atmosphere).



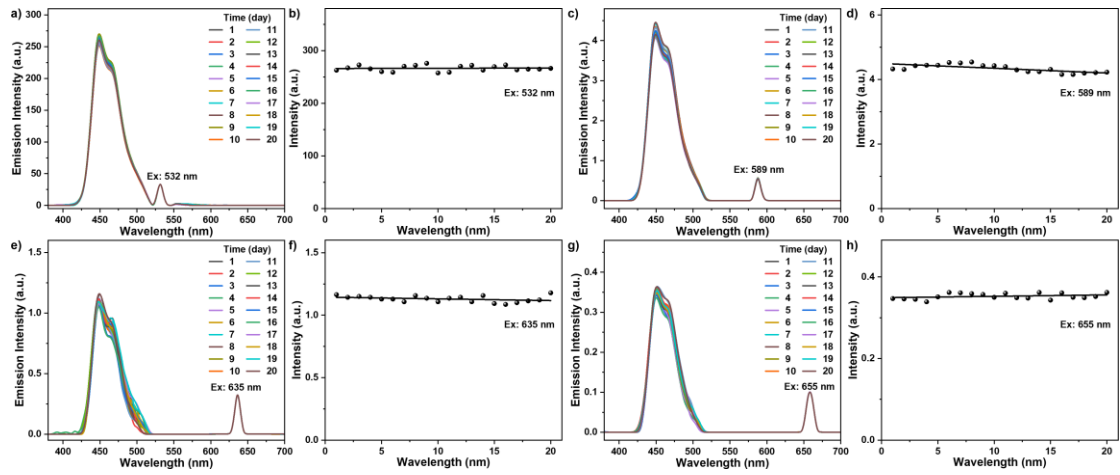


**Fig. S16** At power density at  $968 \text{ mW}\cdot\text{cm}^{-2}$ , the changes of emission spectra and UC intensity of 1/12000 doped microcrystals, under excitation of (a,b) 532 nm, (c,d) 589 nm, (e,f) 635 nm and (g,h) 655 nm through for 20 days (under the air atmosphere).

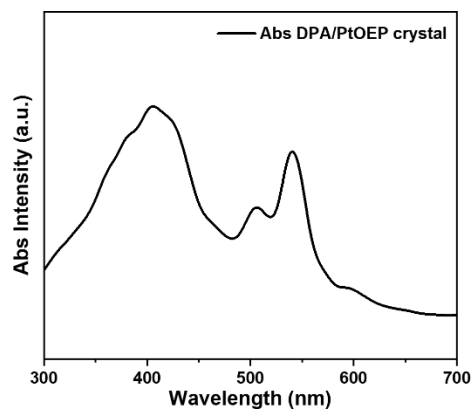


**Fig. S17** Absorption spectrum of the PtOEP-doped (1/12000) DPA microcrystal sample.